RESEARCH ARTICLE | NOVEMBER 19 2019

Shape memory effect and superelasticity in high-strength FeNiCoAlTi single crystals hardened by nanoparticles

Yuriy Chumlyakov; Irina Kireeva; Irina Kuksgauzen; ... et. al

AIP Conference Proceedings 2167, 020064 (2019)
https://doi.org/10.1063/1.5131931

Shape Memory Effect and Superelasticity in High-Strength FeNiCoAlTi Single Crystals Hardened by Nanoparticles

Yuriy Chumlyakov[1,a)], Irina Kireeva[1,b)], Irina Kuksgauzen[1,c)], Vyacheslav Poklonov[1,d)], Zinaida Pobedennaya[1,e)], Irina Bessonova[1,f)], Dmitriy Kuksgauzen[1,g)], Vladimir Kirillov[1,h)], Christian Lauhoff[2,i)], Tomas Niendorf[2,j)], and Philipp Krooß[2,k)]

[1] *Siberian Physical Technical Institute, National Research Tomsk State University, Tomsk, 634050 Russia*
[2] *Institute für Werkstofftechnik, Universität Kassel, Kassel, 34125 Germany*

[a)] chum@phys.tsu.ru
[b)] kireeva@spti.tsu.ru
[c)] Corresponding author: irbas@sibmail.com
[d)] poklonov_vyacheslav@mail.ru
[e)] pobedennaya_zina@mail.ru
[f)] 79516284172@yandex.ru
[g)] kuksgauzen90@gmail.com
[h)] vladk@sibmail.com
[i)] lauhoff@uni-kassel.de
[j)] niendorf@uni-kassel.de
[k)] krooss@uni-kassel.de

Abstract. For [001]-oriented single crystals of Fe-28Ni-17Co-11.5Al-2.5Ti (at %) alloy in tension, it was shown that particles of the γ'-phase with a size of 4–6 nm lead to the appearance of superelasticity, with a strain of ε_{SE} = 4.5% and a shape memory effect of ε_{SME} = 5.9%. Increasing the particle size to 10–12 nm reduces ε_{SE} to 3.6% and ε_{SME} to 3.5%. The paper discusses the causes of the influence of particle size on the reversible strain.

INTRODUCTION

It is known that iron-nickel-based alloys can undergo thermoelastic martensitic transformations (MTs). The conditions for shape memory effect (SME) and superelasticity (SE) in these materials are achieved firstly by alloying with cobalt, which leads to a decrease in the volume change during the MT from the fcc (γ) high-temperature phase into bct (α') tetragonal martensite, due to the invar effect. Secondly, alloying with aluminium, tantalum, niobium and titanium creates conditions for the precipitation of nanosized γ'-phase particles of a complex composition $(NiCoFe)_3AlX$ (X = Ta, Nb, Ti) during ageing. On the one hand, these harden the γ'-phase and impede dislocation slip during the γ–α' MT and on the other hand, they reduce the lattice strain and the value of twinning shear [1–5]. This contributes to the development of thermo-elastic MTs in nanocomposites containing a high volume fraction of γ'-phase particles, which are absent in the particle-free alloys.

The Fe-28Ni-17Co-11.5Al-2.5Ti (at %) alloy represents a group of new FeNiCoAlX (X = Ti, Nb, Ta) alloys in which SME and SE are observed when nanosized particles with $d \le$ 6–10 nm are precipitated in polycrystals and in single crystals. In polycrystals without texture, brittle fracture of nanocomposites occurs immediately after the start of the stress-induced γ–α' MT. Only the creation of a strong ⟨100⟩ texture in FeNiCoAlTaB polycrystals makes it possible to realize the entire crystallographic resource of the γ–α' MT for this orientation (ε_0 = 8.7%) or even to

Proceedings of the International Conference on Advanced Materials with Hierarchical Structure for New Technologies and Reliable Structures 2019
AIP Conf. Proc. 2167, 020064-1–020064-4; https://doi.org/10.1063/1.5131931
Published by AIP Publishing. 978-0-7354-1912-4/$30.00

exceed it with a reversible strain $\varepsilon_{tr} = 13.5\%$ [4]. Fe-28Ni-17Co-11.5Al-2.5X (X = Ti, Nb, Ti) (at %) alloys belong to a new class of non-equiatomic high-entropy fcc alloys which possess SE in a high-strength state, undergo transformations at σ = 1.1 GPa at $T < 77$ K and are characterized by high dissipation energy, which is two and 10 times higher than for Ti-Ni and Cu-Al-Ni alloys respectively [6, 7].

The paper presents new experimental data on the effect of nanosized particles, temperature tests on the thermoelastic γ–α' MT and SME and SE in Fe-28Ni-17Co-11.5Al-2.5Ti (at %) single crystals.

MATERIALS AND METHODS

Ingots for the growth of Fe-28Ni-17Co-11.5Al-2.5Ti (at %) crystals were smelted from the pure elements in an inert gas. The ingot was melted down twice for a uniform distribution of elements along the length of the crystal. Single crystals were grown by the Bridgman method in argon. After growth, the crystals were homogenized in an inert gas for 24 hours (h) at 1573 K. Tension samples had a working section length of 12 mm and a cross section of 2×1.5 mm^2. Crystal orientations were determined using a DRON-3M diffractometer. Mechanical properties were determined on an Instron 5969 testing machine, with a strain rate of 4×10^{-4} s^{-1} in the temperature range from 203 to 573 K. The SME was studied on a specially designed dilatometer with stress variations from 5 to 550 MPa during cooling/heating cycling from 77 to 473 K. Ageing at T = 873 K for 4 h and 8 h was carried out in a helium atmosphere. Before ageing, the samples were quenched from 1573 K, after holding for 1 h. Temperatures of the start M_s and finish M_f of the forward γ–α' MT during cooling and the start of A_s and finish A_f of the reverse α'–γ MT upon heating were determined from the temperature dependence of the electrical resistance $\rho(T)$.

RESULTS AND DISCUSSION

Studies were carried out on [001]-oriented Fe-28Ni-17Co-11.5Al-2.5Ti (at %) single crystals in tension after ageing at 873 K for 4 h (873 K × 4 h) and 8 h (873 K × 8 h). The study of the temperature dependence of the electrical resistance $\rho(T)$ showed that with an increase in the ageing time, there is an increase in the start temperature of the γ–α' MT M_s from 110 to 145 K, for 4 and 8 h ageing respectively.

Figure 1 shows the results of the temperature dependence of axial stresses $\sigma_{0.1}(T)$ for [001]-oriented single crystals of Fe-28Ni-17Co-11.5Al-2.5Ti (at %) alloy aged at T = 873 K for 4 and 8 h. Figures 2 and 3 present the results of the study of the SME and SE respectively.

The $\sigma_{0.1}(T)$ dependence (Fig. 1) has several stages, associated with different deformation mechanisms. Stage I is plastic deformation of the high-temperature phase, where $\sigma_{0.1}$ increases when the test temperature decreases. Stage II is the stress-induced γ–α' MT where, in contrast, $\sigma_{0.1}$ decreases when the test temperature decreases. The maximum in the $\sigma_{0.1}(T)$ dependence corresponds to the M_d temperature, at which the stresses of the plastic flow of the γ'-phase are equal to the stresses of the start of the γ–α' MT. Comparison of the $\sigma_{0.1}(T)$ curves for samples aged for 4 h (Fig. 1, curve *1*) and 8 h (Fig. 1, curve *2*), shows that the value $\alpha = d\sigma_{0.1}/dT$ at stages where $T < M_d$ depends weakly on the ageing time: α(4 h) = 2.9 MPa/K, α(8 h) = 2.4 MPa/K. The stresses $\sigma_{0.1}(M_d)$ also depend weakly on the ageing time.

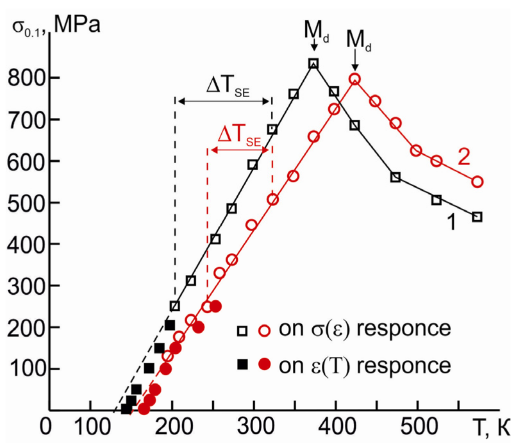

FIGURE 1. Temperature dependence of the axial stresses $\sigma_{0.1}(T)$ for [001]-oriented single crystals of Fe-28Ni-17Co-11.5Al-2.5Ti (at %) alloy aged at T = 873 K for 4 h (curve *1*) and 8 h (curve *2*). Filled points are the stresses obtained by measuring the SME under stress, and open points are the $\sigma_{0.1}$ values obtained under isothermal conditions

Experiments on the study of the SME during cooling/heating under stress from 5 to 550 MPa (Fig. 2), enable the determination of $\sigma_{0.1}(T)$ for the γ–α' transformation at small stress values and the influence of external stresses on the MT temperatures and transformation strain $\varepsilon_{tr} = \varepsilon_{SME}$. The stresses $\sigma_{0.1}$ obtained by measuring the SME under stress, coincide with the extrapolated $\sigma_{0.1}(T)$ curve obtained under isothermal conditions (Fig. 1). Filled points are the stresses obtained by measuring the SME under stress, and open points are the $\sigma_{0.1}$ values obtained under isothermal conditions).

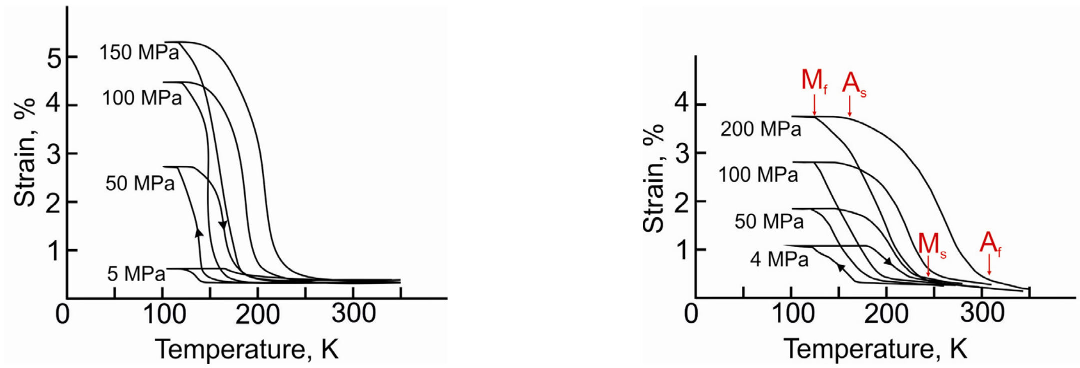

(a) (b)

FIGURE 2. Strain-temperature response obtained during cooling/heating under stress, for [001]-oriented single crystals of Fe-28Ni-17Co-11.5Al-2.5Ti (at %) alloy aged at $T = 873$ K for 4 (a) and 8 h (b)

From Fig. 2 it follows that the $\varepsilon_{tr}(T)$ dependences for 873 K × 4 h and 873 K × 8 h samples with $\sigma > 5$ MPa, differ from each other. Thus, the direct γ–α' MT in the 873 K × 8 h samples, occurs with significant supercooling $\Delta M = M_f - M_s$, while for the 873 K × 4 h crystals, the value of ΔM is lower. The inverse α'–γ MT in the 873 K × 8 h samples, develops in several stages. The A_s temperature at $\sigma > 100$ MPa is low and $A_s < M_s$, which indicates a significant elastic Gibbs energy ΔG_{el} accumulated during the direct transformation. Furthermore, $\Delta G_{el} > 2\Delta G_{diss}$. Here, ΔG_{diss} is the energy dissipation at the γ–α' transformation, which can be estimated from the thermal hysteresis $\Delta T = M_s - A_f$ in experiments on the SME under stress and the stress hysteresis $\Delta\sigma$ in experiments on SE.

Comparison of the $\sigma(\varepsilon)$ curve during unloading and $\varepsilon(T)$ curve for the reverse α'–γ MT (Fig. 3) reveals an analogy in the manifestation of stages in these experiments. In both cases, the reverse transformation begins almost immediately when heating or unloading, and the characteristic stages on the $\sigma(\varepsilon)$ and $\varepsilon(T)$ curves reflect each other. The same correspondence between the stages with different values of $d\sigma/d\varepsilon$ and $d\varepsilon/dT$ is observed at the forward transformation. These results suggest that the processes of forward and reverse transformation under isothermal conditions (SE) and isobaric conditions (SME) occur uniformly, with a change in the volume fraction of martensite which is proportional to the transformation strain ε_{tr} in these two experiments.

In the 873 K × 8 h crystals, compared to the 873 K × 4 h crystals, a number of differences were found. Firstly, the reversible strain in the former was 3.5%, which is less than for the 873 K ×4 h crystals, where $\varepsilon_{SME} = 4.9\%$. Secondly, the forward MT in the 873 K × 8 h crystals occurs with larger values of $d\sigma/d\varepsilon$ and $d\varepsilon/dT$ than in the 873 K × 4 h samples. Thirdly, with an increase in the level of applied stress in the 873 K × 8 h samples, the A_s temperature changes only slightly and the hysteresis $\Delta T^* = A_s - M_f$ decreases, while the hysteresis $\Delta T = A_f - M_s$, in contrast, increases. Fourthly, on the unloading curves, the start of the reverse α'–γ transformation is observed almost at σ_{rev}, close to the stress at the end of the transformation σ_t, with $\sigma_t - \sigma_{rev} = 50$ MPa. Hence, it is clear that in the 873 K × 4 h and 873 K × 8 h crystals, there are differences in ε_{tr}, $d\sigma/d\varepsilon$ and $d\varepsilon/dT$. This is due to the different sizes of the dispersed γ'-phase particles (4–6 or 10–12 nm) precipitated during ageing.

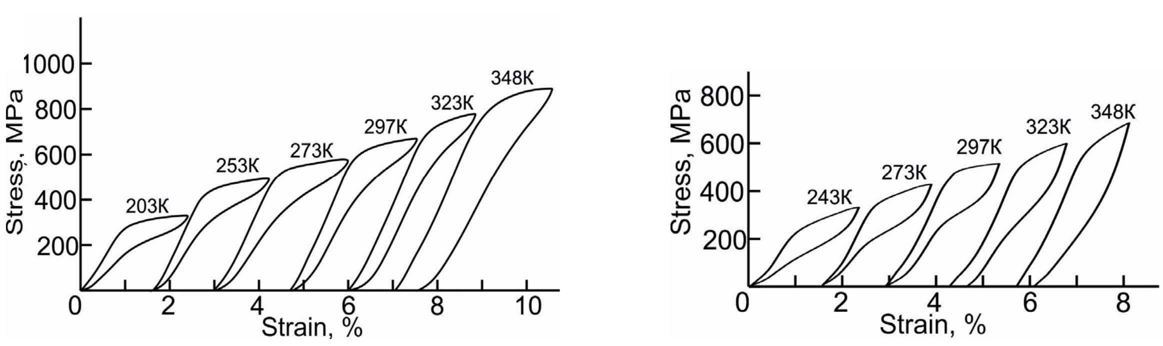

(a) (b)

FIGURE 3. Stress-strain response for [001]-oriented single crystals of Fe-28Ni-17Co-11.5Al-2.5Ti (at %) alloy aged at $T = 873$ K for 4 (a) and 8 h (b)

It can be assumed that with a small particle size of 4–6 nm (873 K × 4 h), particles are inherited by the martensite crystals, while retaining their coherence with the high-temperature phase and martensite. This determines the development of the γ–α' MT primarily in the same system, with low dσ/dε and dε/dT values for the forward transformation. With an increase in particle size to 10–12 nm (873 K × 8 h), it can be assumed that the particles contribute to the local nucleation of martensite variants at the interphase boundaries, with small values of the Schmid factor. In this case, in the regions between particles, the nucleation and growth of martensite variants with maximum Schmid factors occurs. Martensite interaction determines large values of thermal ΔT and stress $\Delta\sigma$ hysteresis and significant supercooling $\Delta M = M_f - M_s$. Fine details of the ε(T) and σ(T) curves, which appear especially noticeable at high stress levels, can be associated with the distribution of particle sizes and their non-uniform distribution over the crystal. The appearance of "tails" at the forward γ-α' transformation, small values of ΔT^* and the presence of a stage with small values of dε/dT at the reverse transformation, can be associated with high resistance on the part of the non-uniform structure. The complete forward MT of the structure with high particle density occurs with significant resistance, and ΔG_{el} increases. A high value of the stored elastic energy ΔG_{el} facilitates the reverse transformation at small values of thermal hysteresis ΔT^*. A similar picture is seen in experiments on the study of SE, for example in 873 K × 4 h crystals. The forward transformation develops in two stages with different values of dσ/dε. In the second stage, with a high value of dσ/dε, the elastic energy increases to complete the transformation. In this case, the reverse transformation during unloading is characterized by low values of $\sigma^* = \sigma_t - \sigma_{rev}$, indicating small energy dissipation at the start of the reverse transformation. Completion of the reverse transformation occurs at significant values of Δσ. The revealed features of the development of the γ–α' MT at high stress values, indicate heterogeneities in the microstructure of the 873 K × 4 h and 873 K × 8 h crystals, which can influence the degradation of functional properties under cyclic loads at different applied stresses and volume fractions of the formed martensite.

CONCLUSION

It is established that the start temperature of the forward MT M_s increases from 110 to 145 K with an increase in the particle size of the γ'-phase from d = 4–6 nm (873 K × 4 h) to d = 10–12 nm (873 K × 8 h).

The transformation strain ε_{tr} (ε_{SME} or ε_{SE}) at the γ–α' MT in [001]-oriented crystals in tension, depends on the particle size d, and is equal to 4.9% and 3.5% for d = 4–6 nm and d = 10–12 nm respectively.

The γ-α' MT at d = 4–6 nm occurs with small values of dσ/dε and dε/dT under isothermal conditions (SE) and isobaric conditions (SME under stress). As d increases to 10–12 nm, the γ–α' MT occurs with significant dσ/dε and dε/dT values.

It is assumed that the features of the development of the γ-α' MT described above, are associated with different mechanisms of martensite-particle interactions. At d = 4–6 nm, the particles retain coherence during the MT, and are inherited by martensite crystals. When d = 10–12 nm, during the γ–α' MT the particles can contribute to local nucleation of martensite on particle-martensite boundaries with a small Schmid factor.

ACKNOWLEDGMENTS

The study of mechanical and functional properties was carried out by a grant from the Russian Science Foundation (project No. 19-49-04101). The structural investigations were supported by the German Research Foundation (Project No. 405372848 (KR 5134/1-1)).

REFERENCES

1. V. V. Kokorin, *Martensite Transformations in Heterogeneous Solid Solutions* (Naukova Dumka, Kiev, 1987).
2. H. Sehitoglu, I. Karaman, X. Y. Zhang, Y. Chumlyakov, and H. J. Maier, Scripta Mater. **44**, 779–784 (2001).
3. Y. I. Chumlyakov, I. V. Kireeva, O. A. Kuts, Y. N. Platonova, I. V. Kukshauzen, D. A. Kukshauzen, V. V. Poklonov, M. Y. Panchenko, and K. A. Reunova, Russ. Phys. J. **58**, 1549–1556 (2016).
4. Y. Tanaka, Y. Himuro, R. Kainuma, Y. Sutou, T. Omori, and K. Ishida, Science **327**, 1488–1490 (2010).
5. A. N. Titenko and L. D. Demchenko, J. Mater. Eng. Perform. **21**, 2525–2529 (2012).
6. C. Zhang, C. Zhu, T. Harrington, L. Casalena, H. Wang, S. Shin, and K. S. Vecchio, Adv. Eng. Mater. **21**, 1800941(9) (2019).
7. W. Abuzaid and H. Sehitoglu, Mater. Des. **160**, 642–651 (2018).